

**Electronic Supplementary Information (ESI) for**

**Fabrication of  $p\text{-Ni}_{0.8}\text{Cu}_{0.2}\text{WO}_4/n\text{-Si}$  heterojunction diode and 1 MHz rectifier operation**

Inseo Kim<sup>1†</sup>, Sora Yun<sup>1†</sup>, Hyun Jae Kim<sup>2,3</sup>, JungYup Yang<sup>1,4</sup>, Kyu Hyoung Lee<sup>2</sup>, Min Suk Oh<sup>3\*</sup>, and Kimoon Lee<sup>1,4\*</sup>

<sup>1</sup>Department of Physics, Kunsan National University, Gunsan 54150, Republic of Korea.

<sup>2</sup>Department of Materials Science and Engineering, Yonsei University, Seoul 03722, Republic of Korea.

<sup>3</sup>Display Research Center, Korea Electronics Technology Institute (KETI), Seongnam 13509, Republic of Korea.

<sup>4</sup>The Institute of Basic Science, Kunsan National University, Gunsan 54150, Republic of Korea.

†These authors contributed equally to this work.

\*Corresponding author: [ohms@keti.re.kr](mailto:ohms@keti.re.kr), [kimoon.lee@kunsan.ac.kr](mailto:kimoon.lee@kunsan.ac.kr)

**S1. Schematic of target synthesis and deposition.**

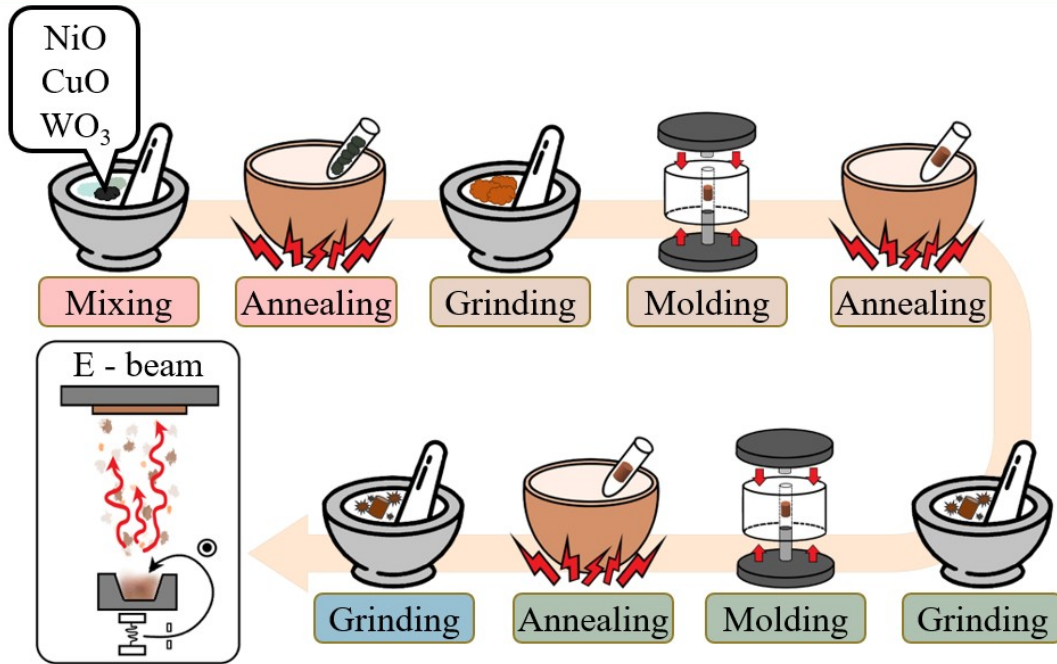


**Figure S1.** The schematic of  $\text{Ni}_{0.8}\text{Cu}_{0.2}\text{WO}_4$  target synthesis process for e-beam evaporation.

## S2. The purity of synthesized target.

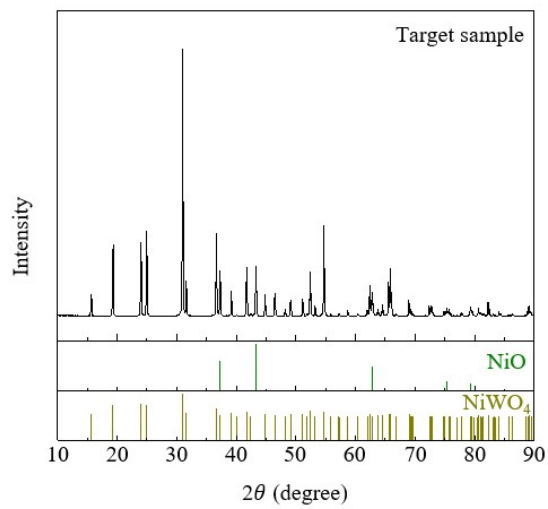


**Figure S2.** The powder XRD pattern for the synthesized target. All the peaks are well indexed only with NiWO<sub>4</sub> and NiO peaks without other secondary phases.

**S3. The ohmic contact behaviours between  $p\text{-Ni}_{0.8}\text{Cu}_{0.2}\text{WO}_4$  and Au.**

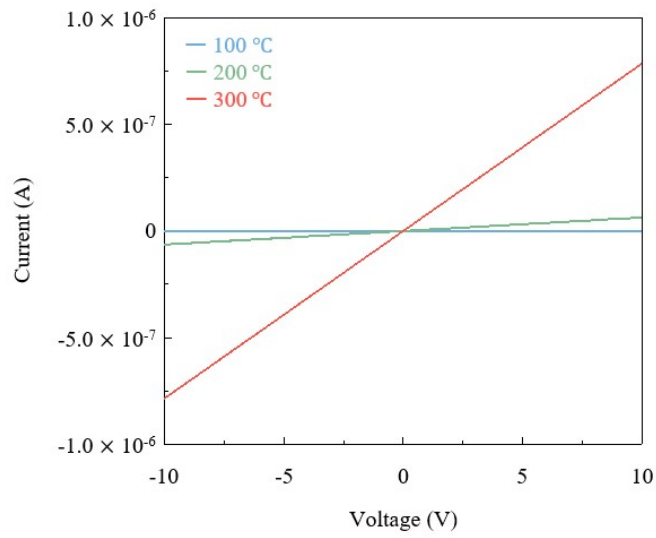


**Figure S3.** The I-V characteristics from Au/ $\text{Ni}_{0.8}\text{Cu}_{0.2}\text{WO}_4$ /Au geometry devices for 100, 200, and 300 °C deposited samples.

**S4. The Raman spectrum analysis.**

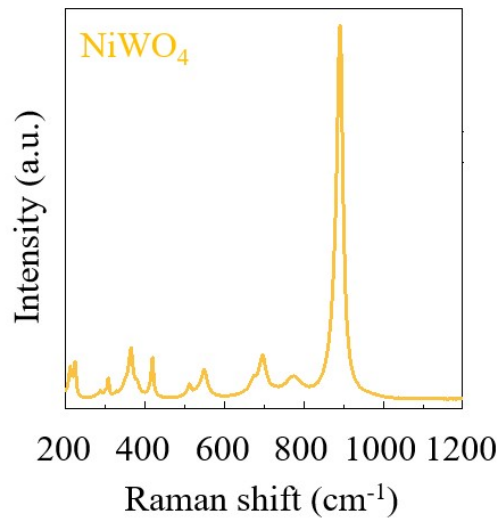


**Figure S4.** The Raman spectrum for the pure NiWO<sub>4</sub> sintered bulk form as reference.

**S5. Optical absorption spectra of  $\text{Ni}_{0.8}\text{Cu}_{0.2}\text{WO}_4$  films.**

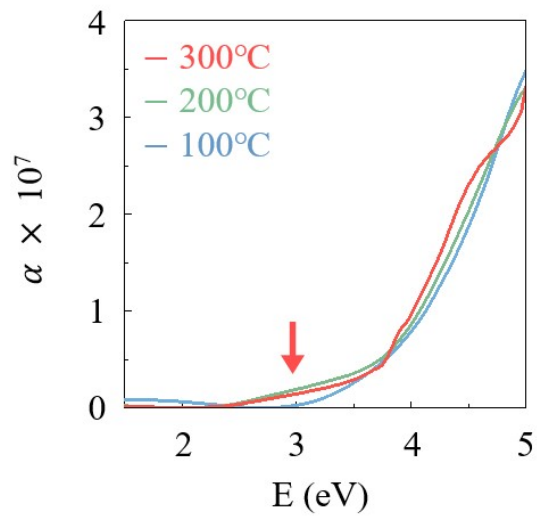


**Figure S5.** The absorption coefficient vs. optical energy ( $E$ ). The shoulder peak is marked by red-arrow.

**S6. Band-diagram picture for  $p\text{-Ni}_{0.8}\text{Cu}_{0.2}\text{WO}_4/n\text{-Si}$  heterojunction.**

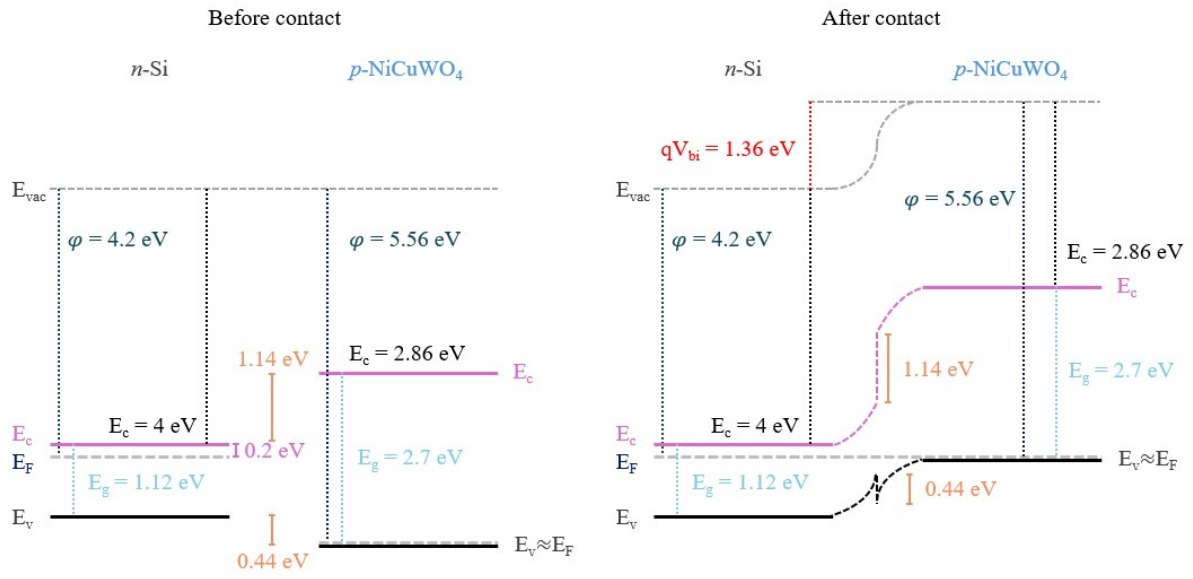


**Figure S6.** The schematic of band-diagram for  $p\text{-Ni}_{0.8}\text{Cu}_{0.2}\text{WO}_4/n\text{-Si}$  heterojunction. The band parameters for  $\text{Ni}_{0.8}\text{Cu}_{0.2}\text{WO}_4$  are referred from our previous work. [*Mater. Horiz.* **11**, 6342 (2024)]

**S7. The current density ( $J$ ) – voltage ( $V$ ) characteristics the  $p\text{-Ni}_{0.8}\text{Cu}_{0.2}\text{WO}_4/n\text{-Si}$  heterojunction diodes.**

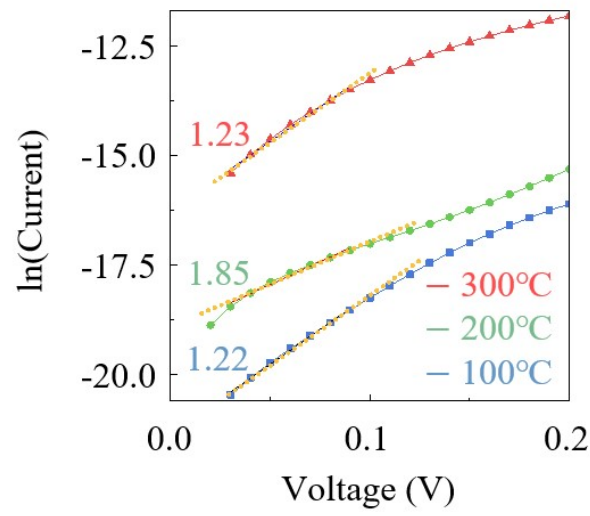


**Figure S7.** The  $\ln J - V$  characteristics for different substrate heating temperature. The idearity factors are obtained based on following equation of  $J = J_s \{ \exp [qV/nkT] - 1 \}$ .



### S8. The half-wave rectifications behavior of the $p\text{-Ni}_{0.8}\text{Cu}_{0.2}\text{WO}_4/n\text{-Si}$ heterojunction diode.

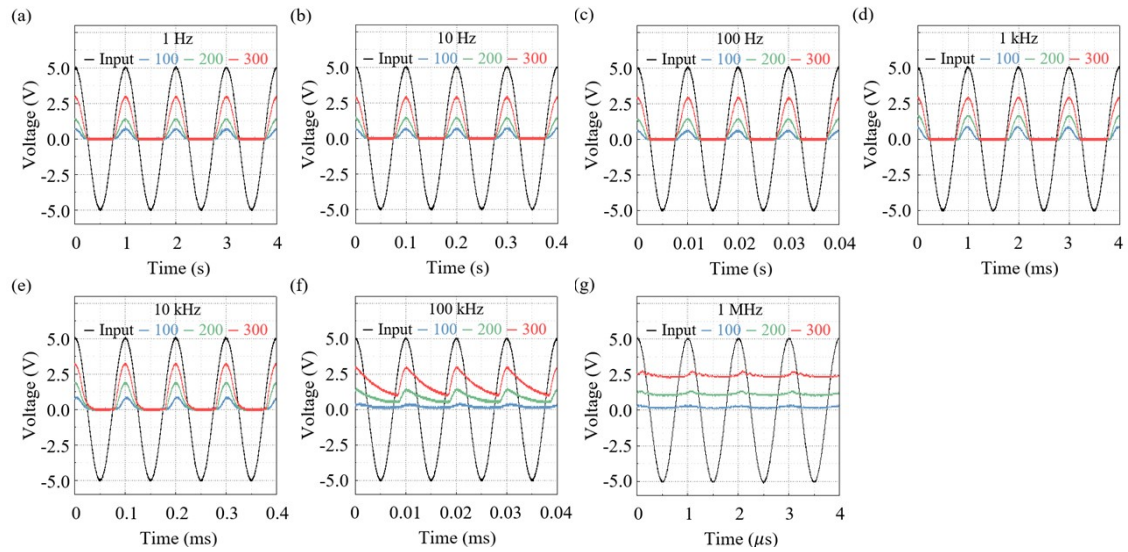


**Figure S8.** The output signals of the half-wave rectification circuit at (a) 1 Hz, (b) 10 Hz, (c) 100 Hz, (d) 1 kHz, (e) 10 kHz, (f) 100 kHz, and (g) 1 MHz when applying a 5 V sinusoidal AC input signal.